1993ApJ...404..620Y

THE ASTROPHYSICAL JOURNAL, 404:620–624, 1993 February 20
© 1993. The American Astronomical Society. All rights reserved. Printed in U.S.A.

THE 6.7 keV IRON LINE DISTRIBUTION IN THE GALAXY

SHIGEO YAMAUCHI AND KATSUJI KOYAMA
Department of Physics, Faculty of Science, Kyoto University, Sakyo-ku, Kyoto, 606-01
Received 1992 June 5; accepted 1992 August 25

ABSTRACT

We have systematically observed the 6.7 keV iron line emission from the Galactic ridge with the X-ray satellite *Ginga*. The volume emissivity of the iron line emission from the Galactic ridge is approximated by an exponential disk model plus an arm component of Galactic radius 4 kpc. The scale height of the Galactic ridge emission is determined to be 100 ± 20 pc. The iron line luminosity from the Galactic ridge is estimated to be $(6.5 \pm 1.3) \times 10^{36}$ ergs s^{-1}, which is $\sim 7\%$ of the 2–10 keV band luminosity. We have also discovered another diffuse emission feature near the Galactic bulge with luminosity of about $(2.8 \pm 0.8) \times 10^{36}$ ergs s^{-1}. This emission is found to be extended to a higher Galactic latitude of more than 5°.

Subject headings: diffuse radiation — Galaxy: structure — X-rays: galaxies

1. INTRODUCTION

The X-ray sky along the Galactic plane exhibits many bright point sources, consisting mainly of neutron star binaries (e.g., Warwick et al. 1985, 1988). In addition to these bright sources, fainter and unresolved X-ray emission was also observed (Worrall et al. 1982; Warwick et al. 1985, 1988). Since the unresolved emission is concentrated near the Galactic inner disk (within $\sim 60°$ of longitude), this is referred to as the Galactic ridge emission (Worrall et al. 1982; Warwick et al. 1985; 1988). However, previous observations of the unresolved emission suffered from the confusion of the bright X-ray sources.

From selected regions of the Galactic ridge, a conspicuous line emission at 6.7 keV was discovered with the *Tenma* satellite (Koyama et al. 1986). Since the 6.7 keV line is attributable to a K-shell transition of helium-like iron (Fe XXV) and the X-ray spectrum is well represented by the thermal bremsstrahlung model with temperatures of $(4–13) \times 10^7$ K, the Galactic ridge X-rays are undoubtedly due to an optically thin hot plasma. Koyama (1989) reported that the equivalent width of the line emission is in the range of 0.5–1 keV which is more than 10 times larger than the majority of bright X-ray sources (Suzuki et al. 1984; Hirano et al. 1986). Therefore, the 6.7 keV iron line should be a better tracer of the optically thin hot plasma than the X-rays in the wide energy band.

We have carried out a survey of the 6.7 keV line emission along the Galactic plane with the *Ginga* satellite and certainly detected an intense 6.7 keV line from the Galactic center, inner Galactic disk, and the Galactic bulge regions. Discovery of the large enhancement of the iron line emission at the Galactic center and its consequence was already reported in separate papers (Koyama et al. 1989; Yamauchi et al. 1990). In this paper, we present the X-ray contour map of the 6.7 keV line intensity and an overall distribution of an optically thin hot plasma in the inner disk of our Galaxy. Throughout this paper, we assume that the distance to the Galactic center is 8.5 kpc.

2. OBSERVATIONS

Extensive scanning observations were carried out with the Large Area Proportional Counters (LAC) on board the *Ginga* satellite (Turner et al. 1989; Makino & ASTRO-C team 1987) from the period of 1987–1990. The FWHM of the LAC field of view is $\sim 1°$ along and 2° perpendicular to the scan path. The total effective area of the LAC is 4000 cm^2 and its energy range is 1–37 keV. The accuracy of the attitude determination is better than 0°.1. Data were taken in the 48 energy channel mode (MPC-1 or MPC-2 mode).

Scan paths were set parallel to the Galactic plane. To increase the statistics and to minimize background fluctuations, multiple scans (three to 14 scans day^{-1}) were performed over the same path with the scan speed of $\sim 1°$ minute^{-1}. The log of observations is summarized in Table 1.

3. ANALYSIS AND RESULTS

3.1. *Overall Distribution of the 6.7* keV *Line*

The multiple scan data were folded azimuthally and sliced at 0°.4–4°.0 intervals. Then the X-ray spectrum for each position was constructed. Non–X-ray events and the cosmic X-ray background were subtracted using the method given by Awaki et al. (1991). In order to determine the iron line intensity, the X-ray spectra in the 4.5–14 keV energy band were fitted with a model consisting of a thermal bremsstrahlung component, a narrow emission line, and photoelectric absorption. Free parameters are normalization and temperature of the thermal bremsstrahlung emission, intensity, and energy of the line emission, and hydrogen column density. The Gaunt factor of the thermal bremsstrahlung and the cross sections for photoelectric absorption were taken from Gould (1980) and from Morrison & McCammon (1983), respectively. This model generally gives acceptable fit except for the regions where the confusion of bright binary X-ray sources is significant. The temperature and equivalent width of the 6.7 keV line are found to be in the range of 5–10 keV and in the range of 0.5–1.0 keV, respectively.

To demonstrate visually, we made the intensity contour map of the 6.7 keV line in Figure 1. We used the triangle grid method with typical grid sizes of $\sim 1°$ and 0°.5 for the Galactic ridge and center regions, respectively. Since the number of scan paths in the regions of the map of $-60° < l < -6°$, $11° < l < 20°$, and $40° < l < 60°$ is limited, these regions are blank in the two-dimensional contour map. Strong Galactic center source is demonstrated in this figure. However, since this contour map is not deconvolved with the LAC collimator response, the tilted structure reported by Yamauchi et al. (1990) is not clear.

The 6.7 keV line distribution along the Galactic plane (Galactic latitude $\sim 0°$) is given in Figure 2 together with the

© American Astronomical Society • Provided by the NASA Astrophysics Data System

1993ApJ...404..620Y

TABLE 1

Ginga OBSERVATION OF OPTICALLY THIN HOT PLASMA

DATE	SCAN AREA l	SCAN AREA b	MODE/TIME RESOLUTION	SCAN SPEED (degree per minute)	NUMBER OF SCANS
1987 Aug 24–25	288° ↔ 322°	−0°.2	MPC-1/0.5, 4, 16 s	0.53	12
1987 Aug 25	287 ↔ 322	1.3	MPC-1/4 s	0.53	7
1987 Oct 6	20 ↔ 40	0.2	MPC-1/4 s	0.95	9
1987 Oct 7	20 ↔ 40	1.7	MPC-1/4 s	0.95	8
1987 Oct 8	20 ↔ 40	−2.8	MPC-1/4 s	0.95	8
1987 Oct 9	20 ↔ 40	−0.5	MPC-1/4 s	0.95	9
1988 Mar 17	345 ↔ 20	0.5	MPC-1/4 s	1.38	8
1988 Mar 19–20	356 ↔ 15	3.4	MPC-1/16 s	0.42	8
1988 Mar 21	355 ↔ 16	5.1	MPC-1/4 s	0.53	8
1988 Mar 22	357 ↔ 15	2.0	MPC-1/4 s	0.42	7
1988 Mar 23	0 ↔ 16	−3.5	MPC-1/4 s	0.42	8
1988 Apr 6–7	304 ↔ 340	0.6	MPC-2/2 s	0.63	6
1988 Sep 12–13	22 ↔ 48	−0.3	MPC-2/2 s	0.74	14
1988 Sep 13–14	35 ↔ 60	0.6	MPC-2/2 s	0.74	11
1989 Mar 3–4	324 ↔ 343	0.4	MPC-2/2 s	0.43	12
1989 Apr 1	352 ↔ 8	−1.1	MPC-1/16 s	0.64	5
1989 Apr 2	352 ↔ 8	−0.6	MPC-1/16 s	0.64	4
1989 Apr 5	352 ↔ 8	1.7	MPC-1/4 s	0.95	4
1989 Apr 5	352 ↔ 8	2.1	MPC-1/4 s	0.95	4
1989 Apr 6	352 ↔ 8	−2.1	MPC-1/4 s	1.38	8
1989 Apr 7	355 ↔ 5	−6.9	MPC-1/16 s	0.64	5
1989 Apr 8	355 ↔ 5	−6.3	MPC-1/16 s	0.64	3
1989 Apr 9	356 ↔ 4	−9.9	MPC-1/4 s	0.64	3
1989 Apr 9	356 ↔ 4	−9.6	MPC-1/4 s	0.64	3
1990 Mar 24–25	356 ↔ 4	9.5	MPC-1/16 s	0.64	6
1990 Mar 26	356 ↔ 4	12.3	MPC-1/16 s	0.64	8
1990 Mar 27	356 ↔ 4	14.9	MPC-1/16 s	0.64	8

scan profile in the 1.1–18.5 keV energy band. Note that the scan profile is not fully resolved in Galactic latitude, because the LAC beam size is 2° (FWHM) in the direction of latitude. This figure is similar to that reported previously (Koyama et al. 1989). However, we have extended further the data point and made minor corrections due to the contribution of cataloged point source. This figure demonstrates clear difference between the X-ray sky of the 6.7 keV line and that of the continuum energy band.

3.2. *Model of Galactic Ridge Emission*

To evaluate the 6.7 keV line distribution quantitatively, we modeled the two-dimensional distribution of the 6.7 keV line flux. We assumed that the volume emissivity of 6.7 keV line (η) is given as a function of the galactocentric radius (R) and the distance from the Galactic plane (z). Since the 6.7 keV line distribution shows tail structure to a large longitude, we applied an exponential disk model

$$\eta(R, z) = \eta_d \exp\left(-\frac{R}{R_d}\right) \exp\left(-\frac{|z|}{z_s}\right) \text{ (photons s}^{-1}\text{ cm}^{-3}\text{)} \quad (1)$$

The surface brightness of the 6.7 keV line [$S(l, b)$] is evaluated by the path integral of the volume emissivity along the line of sight

$$S(l, b) = \int_0^\infty \frac{\eta(R, z)}{4\pi}\, ds \text{ (photons s}^{-1}\text{ cm}^{-2}\text{ sr}^{-1}\text{)}\,. \quad (2)$$

After convolving the surface brightness distribution [$S(l, b)$] with the LAC collimator response function, we fitted this model function to the observed flux. Free parameters are

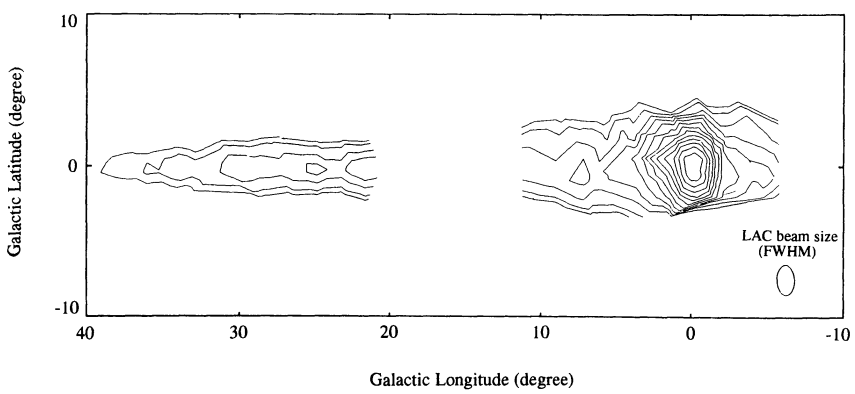

FIG. 1.—Two-dimensional distribution of 6.7 keV iron line emission in $-6° \le l \le 11°$ and $20° \le l \le 40°$ regions. The contour levels are 1.0, 1.2, 1.6, 2.0, 2.5, 3.2, 4.0, 5.0, 6.3, 7.9, 10.0, 12.6, and 15.8 photons s^{-1} (LAC beam)$^{-1}$.

© American Astronomical Society • Provided by the NASA Astrophysics Data System

1993ApJ...404..620Y

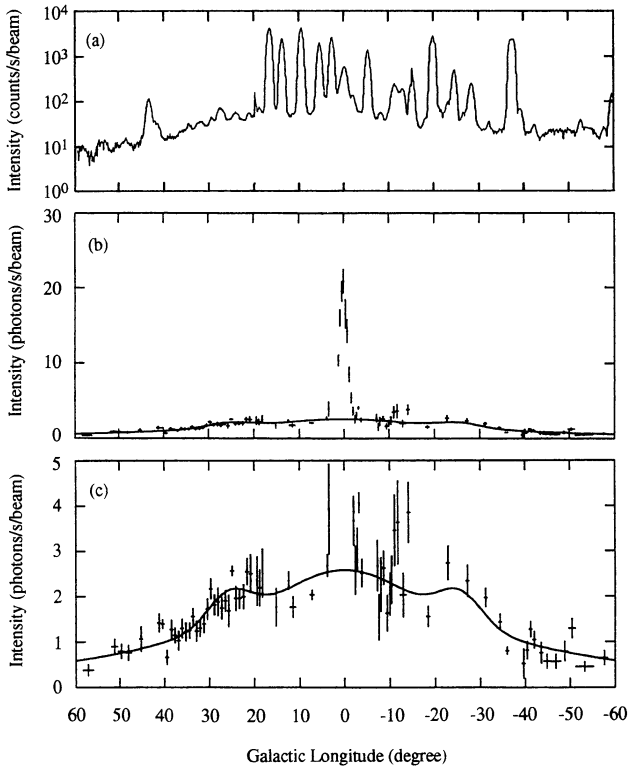

FIG. 2.—Intensity distribution of the 1.1–18.5 keV band (*a*) and the 6.7 keV iron line (*b*) along the Galactic plane. Enlarged plot of (*b*) is given in (*c*). The solid line in (*b*)–(*c*) is the intensity profile expected from the galactic disk plus "4-kpc arm" model (see text and Table 2). Vertical error bars are at 1 σ level.

volume emissivity; (η_d), radius (R_d) and scale height (z_s). In the fitting, we used all the data listed in Table 1 except for the Galactic center region of $|l| < 10°$. This model is rejected with the χ^2 value of 368.4 with 129 degrees of freedom. In fact, we found systematic excess emission at around $l = \pm 30°$. Therefore we added a "Galactic arm" component at this position assuming a Gaussian shape emissivity

$$\eta(R, z) = \left\{\eta_d \exp\left(-\frac{R}{R_d}\right) + \eta_a \exp\left(-\frac{(R - R_a)^2}{2w^2}\right)\right\} \times \exp\left(-\frac{|z|}{z_a}\right) \text{(photons s}^{-1}\text{ cm}^{-3}\text{)} \quad (3)$$

The first and the second terms correspond to the Galactic disk and the Galactic arm components, respectively. Thus, additional free parameters are volume emissivity of the arm component (η_a), radius of arm (R_a), and arm width (w). Although this model is still not acceptable with χ^2 value of 246.8 (126 d.o.f.), the improvement of χ^2 value of 121.6 indicates that the arm component is statistically significant with a confidence level of more than 99%. The best-fit model parameters are listed in Table 2, while the best-fit model distribution along the Galactic plane is shown by the solid line in Figures 2*b*–2*c*. The position of the "Galactic arm" is derived to be at 4 kpc from the Galactic center, and hence may be referred to as the "4 kpc arm." This region coincides with the "5 kpc arm" of CO (named when the nominal distance of the Galactic center was 10 kpc). The estimated 6.7 keV line luminosities from the

TABLE 2

RESULT OF MODEL[a] FITTING TO THE GALACTIC RIDGE EMISSION

Parameter	Value
η_d (photons s^{-1} cm^{-3})	$(1.2 \pm 0.1) \times 10^{-21}$
R_d (kpc)	3.6 ± 0.2
η_a (photons s^{-1} cm^{-3})	$(2.6 \pm 0.5) \times 10^{-22}$
R_a (kpc)	4.0 ± 0.2
w (kpc)	0.51 ± 0.12
z_s (kpc)	0.10 ± 0.02
Reduced χ^2/d.o.f.	1.958/126

NOTE.—Quoted errors are single-parameter 90% confidence limits.

[a] Exponential disk model + galactic arm emission model

$$\eta(R, z) = \left\{\eta_d \exp\left(-\frac{R}{R_d}\right) + \eta_a \exp\left(-\frac{(R - R_a)^2}{2w^2}\right)\right\} \times \exp\left(-\frac{|z|}{z_a}\right).$$

Galactic disk and "4 kpc arm" are $(6.1 \pm 1.3) \times 10^{36}$ ergs s^{-1} and $(4.5 \pm 1.6) \times 10^{35}$ ergs s^{-1}, respectively.

3.3. *Excess Emissions near the Galactic Center*

The iron line intensity distribution near the Galactic bulge region $3° \leq |l| \leq 7°$ is plotted in Figure 3*a* as a function of the Galactic latitude. The solid lines are the model profile of the Galactic ridge emission at $|l| = 3°$ and 7°, which is determined by the equation (3) with the best-fit parameters given in Table 2. We find clear excess above the ridge emission model as is given in Figure 3*a*. Since this region is confusion-free from the Galactic center emission as was determined by Yamauchi et al. (1990), the excess emission would be a new component of the Galactic diffuse emission. Here we call this as the Galactic

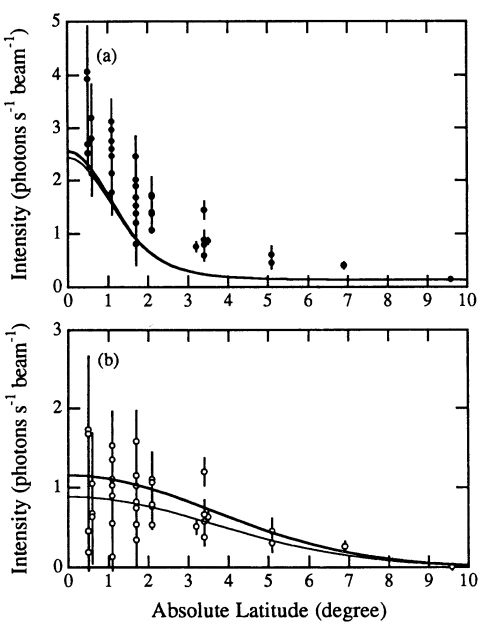

FIG. 3.—(*a*) Iron line flux as a function of the Galactic latitude near the Galactic bulge region of $3° \leq |l| \leq 7°$. Solid thick and thin lines indicate the model distribution of the galactic ridge at $|l| = 3°$ and 7°, respectively. (*b*) The excess flux above the ridge model. The solid thick and thin lines are the best-fit model of Galactic bulge emission at $|l| = 3°$ and 7°, respectively (see text).

© American Astronomical Society • Provided by the NASA Astrophysics Data System

1993ApJ...404..620Y

TABLE 3

RESULT OF MODEL[a] FITTING TO THE GALACTIC BULGE EMISSION

Parameter	Value
S_0 (photons s^{-1} cm^{-2} sr^{-1})	0.55 ± 0.10
x	$12° \pm 2°$
y	$5° \pm 1°$
Reduced χ^2/d.o.f.	2.436/24

NOTE.—Quoted errors are single-parameter 90% confidence limits.

[a] Surface brightness model

$$S(l, b) = S_0 \times \exp\left[-\left(\frac{l}{x}\right)^2 - \left(\frac{b}{y}\right)^2\right].$$

bulge emission. The two-dimensional scan data of the bulge region, after subtracting the ridge component, are fitted to the model with a surface brightness of

$$S(l, b) = S_0 \exp\left[-\left(\frac{l}{x}\right)^2 - \left(\frac{b}{y}\right)^2\right] (\text{photons s}^{-1}\text{ cm}^{-2}\text{ sr}^{-1}) . \quad (4)$$

Free parameters are the normalization (S_0) and the scale parameters (x, y). The fitting was unacceptable with the reduced χ^2 value of 2.436 (24 d.o.f.). However, this simple model is still useful to estimate the overall distribution and the total flux of the Galactic bulge emission. Thus we have listed the best-fit parameters in Table 3. The best-fit model of the bulge component is plotted in Figure 3*b*. The total iron line luminosity of the bulge component is estimated to be $(2.8 \pm 0.8) \times 10^{36}$ ergs s^{-1}.

4. DISCUSSION

4.1. *The Galactic Ridge Emission*

Koyama et al. (1986) and Koyama (1989) reported that the X-ray spectra of the Galactic ridge emission are represented by a thermal emission with temperatures of 4–13 keV and an intense 6.7 keV iron line emission consistent with the cosmic abundance. *Ginga* spectra of the Galactic ridge, free from confusion of cataloged X-ray sources, show the same characteristics.

The total iron line flux in the Galactic ridge (excluding the bulge component) is $\sim 7 \times 10^{36}$ ergs s^{-1}, while that of the 2–10 keV X-ray band is $\sim 10^{38}$ ergs s^{-1} (Worrall et al. 1982; Warwick et al. 1985; Koyama et al. 1986). Thus the luminosity ratio of the 6.7 keV line to the 2–10 keV band is $\sim 7\%$.

Possible origin of the Galactic ridge iron emission would be an integrated emission of unresolved faint point-sources which have a strong 6.7 keV line in their spectra. White dwarf binaries (cataclysmic variables hereafter CVs) and late-type star binaries such as RS CVn and W UMa type are known to have thin thermal spectra. However, recent high-quality *Ginga* spectra suggest that the iron line equivalent width for these objects is generally smaller than that expected from the plasma of cosmic abundance (Tsuru et al. 1989, 1992; Doyle et al. 1991; Ishida et al. 1991; Ishida 1992). The plasma temperature of CVs is higher than that of the Galactic ridge emission (Ishida et al. 1991, 1992; Ishida 1992). Furthermore the scale height of white dwarfs and late-type stars are larger than that of the ridge emission (Allen 1973). Therefore, we conclude that CVs and RS CVn stars are not a major contributor to the Galactic ridge emission. Ottmann & Schmitt (1992) also concluded that RS CVn systems are unable to account for the Galactic ridge iron emission.

Another candidate would be young supernova remnants (SNRs) and star-forming regions. For comparison, the number distribution of radio SNRs (Green 1988) and the CO line flux distribution (Dame et al. 1987) along the Galactic plane are given in Figures 4*b*–4*c*. The distribution of CO line flux may be a tracer of active star-forming regions, while that of radio SNRs traces regions of supernova explosions. Since the survey observation of the radio SNRs near the Galactic center was biased by a higher background level, we cannot compare details on the Galactic center region. Thus we may conclude that the iron line distribution is similar to those of SNRs and CO emissions. The scale height of $(1.0 \pm 0.2) \times 10^2$ pc for 6.7 keV line is larger than those of CO and SNRs, but is marginally consistent. Therefore we suggest that the 6.7 keV line emitting plasma has close relation to the active regions of the star-formation and/or supernova explosion.

Some star-forming regions are known to emit a strong 6.7 keV line (Agrawal et al. 1986; Koyama 1987; Kuriyama et al. 1992; Koyama et al. 1992a; Yamauchi & Koyama 1993), but

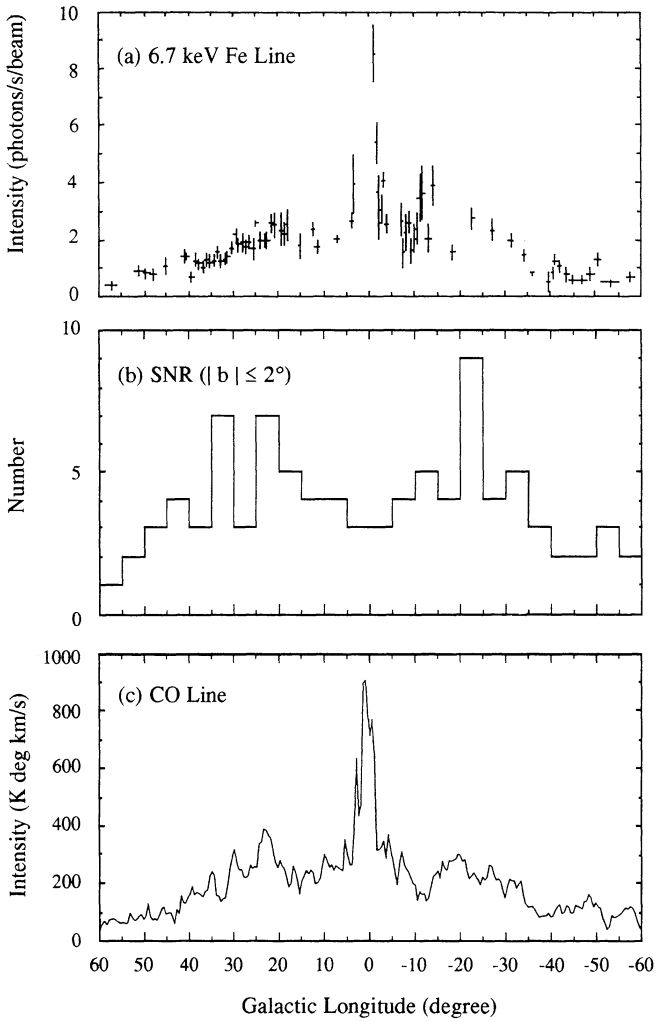

FIG. 4.—(*a*) Distribution of the 6.7 keV iron line intensity, (*b*) number of radio SNRs within $|b| \leq 2°$ (Green 1988), and (*c*) the CO line intensity (Dame et al. 1987) along the Galactic plane.

© American Astronomical Society • Provided by the NASA Astrophysics Data System

1993ApJ...404..620Y

the flux is smaller than that expected from the cosmic abundance. Furthermore, available data of the 6.7 keV line flux from these regions are very limited to make a quantitative estimate of the contribution to the Galactic ridge emission.

On the other hand, the mean equivalent width of the iron line from SNRs, although data are also still not sufficient, is in the range of 0.5–1.5 keV. Koyama, Ikeuchi, & Tomisaka (1986) proposed that, in the Galactic ridge, there would be more than 10^3 unidentified SNRs, which have rather low surface brightness in X-rays as well as in radio bands, and hence they were not detected previously. One example of such SNRs would be RX 04591+5197, a new SNR detected with the soft X-ray telescope onboard *ROSAT* (Pfeffermann, Aschenbach, & Predehl 1991). This SNR was also detected in the hard X-ray band with the *Ginga* satellite (Koyama et al. 1992b). If we assume that many radio-weak SNRs similar to RX 04591+5197 are lying in the Galactic ridge, they would be hardly detected as each SNR by radio band but would contribute to the diffuse X-rays and the 6.7 keV lines. Since the soft X-rays from the SNRs in the Galactic ridge would be largely absorbed, diffuse X-rays from the integrated emission of the SNRs would be rather hard as that really observed. However, there is one serious problem. Since SNRs with low surface brightness would be expanding into a locally tenuous medium, iron atoms in the SNRs would be in ionization nonequilibrium. Then the energy of iron line is lower than 6.7 keV. To solve this problem, we need further systematic study of iron line structure of SNRs.

4.2 *Galactic Bulge Emission*

We have discovered extended iron line emission near the Galactic bulge. The overall spectral feature is similar to those of the Galactic ridge emission. In particular, we note that the equivalent width of the iron line is in the range of 0.5–1 keV, which suggests that the iron abundance is cosmic value (Masai 1984). Can we apply the same discussion as is given in § 4.1) for the origin of the bulge emission? Since most of the star in the Galactic bulge would belong to the old populations, and hence Type Ia supernova explosion would be preferable than Type II. Then the iron line abundance must be far larger than the cosmic abundance. However, it may be in conflict to the observational fact.

Koyama et al. (1989) and Yamauchi et al. (1990) have reported that there is a large enhancement of 6.7 keV iron line emission associated with a thin hot plasma at the Galactic center. They pointed out that the temperature of the Galactic center plasma is higher than that bounded by the Galactic gravity. Therefore the hot gas would escape from the Galactic center to the Galactic bulge. This would be another possibility for the origin of the Galactic bulge emission.

The authors are grateful to all members of the *Ginga* team. Data analyses were carried out with the FACOM M380 computer at the High Energy Physics Laboratory of Nagoya University. This work was supported in part by the Scientific Research Fund of the Japanese Ministry of Education, Science, and Culture.

REFERENCES

Agrawal, P. C., Koyama, K., Matsuoka, M., & Tanaka, Y. 1986, PASJ, 38, 723
Allen, C. W. 1973, in Astrophysical Quantities (3d ed.; London: Athlone)
Awaki, H., Koyama, K., Kunieda, H., Tawara, Y., & Takano, S. 1991, ApJ, 366, 88
Dame, T. M., et al. 1987, ApJ, 322, 706
Doyle, J. G., et al. 1991, MNRAS, 248, 503
Gould, R. J. 1980, ApJ, 238, 1026
Green, D. A. 1988, Ap&SS, 148, 3
Hirano, T., Hayakawa, S., Nagase, F., Masai, K., & Mitsuda, K. 1987, PASJ, 39, 619
Ishida, M. 1992, Ph.D. Thesis, University of Tokyo
Ishida, M., Makishima, K., Ohashi, T., Osborne, J. P., & Watson, M. G. 1992, in Proc. Frontiers of X-Ray Astronomy, ed. Y. Tanaka & K. Koyama (Tokyo: Universal Academy), 283
Ishida, M., Silber, A., Bradt, H. V., Remillard, R. A., Makishima, K., & Ohashi, T. 1991, ApJ, 367, 270
Koyama, K. 1987, PASJ, 39, 245
———. 1989, PASJ, 41, 665
Koyama, K., Asaoka, I., Kuriyama, T., & Tawara, Y. 1992a, PASJ, in press
Koyama, K., Awaki, H., Kunieda, H., Takano, S., Tawara, Y., Yamauchi, S., Hatsukade, I., & Nagase, F. 1989, Nature, 339, 603
Koyama, K., Makishima, K., Tanaka, Y., & Tsunemi, H. 1986, PASJ, 38, 121
Koyama, K., Ikeuchi, S., & Tomisaka, K. 1986, PASJ, 38, 503
Koyama, K., et al. 1992b, in preparation
Kuriyama, T., Koyama, K., Tawara, Y., & Asaoka, I. 1992, in Proc. Frontiers of X-ray Astronomy, ed. Y. Tanaka & K. Koyama (Tokyo: Universal Academy), 277
Makino, F., & ASTRO-C team 1987, Ap. Letters Comm., 25, 223
Masai, K. 1984, Ap&SS, 98, 367
Morrison, R., & McCammon, D. 1983, ApJ, 270, 119
Ottmann, R., & Schmitt, J. H. M. M. 1992, A&A, 256, 421
Pfeffermann, E., Aschenbach, B., & Predehl, P. 1991, A&A, 246, L28
Suzuki, K., Matsuoka, M., Inoue, H., Mitsuda, K., Ohashi, T., Tanaka, Y., Hirano, T., & Miyamoto, S. 1984, PASJ, 36, 761
Tsuru, T., et al. 1989, PASJ, 41, 679
Tsuru, T., Makishima, K., Ohashi, T., Sakao, T., Pye, J. P., Williams, O. R., Barstow, M. A., & Takano, S. 1992, MNRAS, 255, 192
Turner, M. J. L., et al. 1989, PASJ, 41, 345
Warwick, R. S., Norton, A. J., Turner, M. J. L., Watson, M. G., & Willingale, R. 1988, MNRAS, 232, 551
Warwick, R. S., Turner, M. J. L., Watson, M. G., & Willingale, R. 1985, Nature, 317, 218
Worrall, D. M., Marshall, F. E., Boldt, E. A., & Swank, J. H. 1982, ApJ, 255, 111
Yamauchi, S., Kawada, M., Koyama, K., Kunieda, H., Tawara, Y., & Hatsukade, I. 1990, ApJ, 365, 532
Yamauchi, S., & Koyama, K. 1993, ApJ, in press

© American Astronomical Society • Provided by the NASA Astrophysics Data System